Decentralized Dynamic State Estimation for Multi-Machine Power Systems with Non-Gaussian Noises: Outlier Detection and Localization ⋆

Bogang Qu [a], Zidong Wang [b], Bo Shen [c,d,*], Hongli Dong [e,f,g]

[a] *College of Automation Engineering, Shanghai University of Electric Power, Shanghai, 200090, China.*

[b] *Department of Computer Science, Brunel University London, Uxbridge, Middlesex, UB8 3PH, United Kingdom.*

[c] *College of Information Science and Technology, Donghua University, Shanghai 201620, China.*

[d] *Engineering Research Center of Digitalized Textile and Fashion Technology, Ministry of Education, Shanghai 201620, China.*

[e] *Artificial Intelligence Energy Research Institute, Northeast Petroleum University, Daqing 163318, China.*

[f] *Heilongjiang Provincial Key Laboratory of Networking and Intelligent Control, Northeast Petroleum University, Daqing 163318, China.*

[g] *Sanya Offshore Oil & Gas Research Institute, Northeast Petroleum University, Sanya 572024, China.*

Abstract

In this paper, the decentralized dynamic state estimation (DSE) problem is investigated for a class of multi-machine power systems with non-Gaussian noises and measurement outliers. A model decoupling approach is adopted to facilitate the decentralized DSE for large-scale power systems. The particle filtering technique plays a key role in the developed DSE scheme with aim to tackle the nonlinearities and the non-Gaussian noises. To mitigate the negative impact from the measurement outliers on the DSE performance, a novel sliding-window-based online algorithm is proposed to detect and further locate the possible outliers based on the historical measurement data. Specifically, some criteria are constructed to i) determine whether a newly arriving measurement vector is contaminated by measurement outliers and ii) locate the abnormal components of such a vector. A conditional posterior Cramér-Rao lower bound is derived to evaluate the estimation performance of the proposed DSE algorithm. Finally, simulation experiments are carried out on the IEEE-39 bus system to verify the effectiveness of the proposed DSE algorithm under the non-Gaussian noises and the measurement outliers.

Key words: Multi-machine power systems, decentralized state estimation, non-Gaussian noise, particle filter, outlier detection and localization.

1 Introduction

Recently, the situational awareness of the power systems based on the dynamic state estimation (DSE) techniques has stirred an ever-increasing research interest, see e.g. [11, 29]. Since the first introduction of the DSE algorithm for power systems in the early 1970s [7], fruitful results have appeared in the literature, see e.g. [8, 19, 29, 31]. Note that most available DSE schemes are executed in a *centralized* manner, and such a manner would suffer from excessively high consumption of communication/computing resources especially when the power grid is scaled up [14]. To deal with this issue, the so-called *decentralized* DSE scheme has been put forward with the aid of model decoupling technique, see e.g. [11, 23, 28] for some representative works. The merits of the decentralized DSE scheme lie in that it only requires the local states (of the corresponding generation unit) to be estimated [20]. Moreover, the maintainability of the power systems can be improved since the local state estimation facilitates the isolation and localization of possible errors/faults within the individual generation unit [23].

Up to now, the Kalman-filter-based approaches have been widely applied in the context of DSE research for power systems, see e.g. [11, 19] for the extended Kalman filtering (EKF) algorithms and [23] for the unscented Kalman filtering (UKF) algorithms. Note that the calculation of the Jacobian matrix in the EKF algorithm often hinder its practical application especially when the system possess high-degree of nonlinearity [23]. As for the UKF approach, the limited number of sigma points and the constraints in the application of the Cholesky decomposition also make it difficult to extend to actual power systems especially in the presence of abnormal measurements and/or complex noise covariance [8]. It should be pointed out that most existing DSE-related results have been obtained on an underlying assumption that the noises follow strict Gaussian distributions, and such an assumption is often unrealistic because of the ever-increasing complexity of the environmental noises. All these facts have necessitated the imperative need to look into the DSE issues for power systems with nonlinearity/non-Gaussianity, and this constitutes the first motivation of our study.

Recently, the experiments conducted by the Pacific

⋆ This work was supported in part by the National Natural Science Foundation of China under Grants 61933007, U21A2019 and 62273088, the Program of Shanghai Academic/Technology Research Leader of China under Grant 20XD1420100, the Hainan Province Science and Technology Special Fund of China under Grant ZDYF2022SHFZ105, the Royal Society of the UK, and the Alexander von Humboldt Foundation of Germany.

* Corresponding author.

Email addresses: bogangqu@163.com (Bogang Qu), Zidong.Wang@brunel.ac.uk (Zidong Wang), bo.shen@dhu.edu.cn (Bo Shen), shiningdhl@vip.126.com (Hongli Dong).

Northwest National Laboratory [26] and the synchronized voltage measurements collected from the Indian synchrophasor network [1] have demonstrated that the measurement noises of the phasor measurement unit (PMU) follow logistic or log-normal distributions. In addition, it has been reported in [25] that the stochastic power flows caused by the penetration of renewable energy generations obey non-Gaussian distributions. All these facts have indicated that the widely used Kalman-filter-based DSE algorithms may no longer be applicable. In this regard, the particle filtering (PF) algorithm appears to be an effective yet reliable approach in dealing with the non-Gaussianity and nonlinearity of the power systems. It should be pointed that the computational efficiency of the PF algorithm is always one of the major issues for its applications in power systems, and the model decoupling technique of the power systems provides a possible solution to such an issue.

In practical power systems, the PMU measurements could be contaminated by outliers due to the unpredictable instrument failures, communication impulses and/or intended cyber-attacks [1, 29]. These outliers, if not dedicatedly tackled, would large affect the DSE performance and even invalidate the estimation algorithms due to the outlier-induced abnormal innovations. So far, several outlier detection strategies have been proposed in the literature to restrain the adverse effects from measurement outliers, see e.g. [10,12,17,18,32]. It should be pointed out that the establishment of these strategies relies heavily on the sufficient knowledge of the outliers (e.g. occasionality, probability, types and/or intermittency). Unfortunately, in the context of actual power systems, it is somehow too strict and even unreasonable to assume that the prior knowledge of measuring outliers is known. Moreover, the limited memory capacity and computing resource of the practical power systems also pose higher requirements on the efficiency of the outlier detection algorithm. As such, it makes practical sense to devise an outlier detection scheme which is free from the influences of prior knowledge of measurement outliers and is also suitable for online application, and this gives rise to another motivation of the current study.

Motivated by the above discussions, in this paper, we endeavor to investigate the decentralized DSE problem for power systems subject to non-Gaussian noises and measurement outliers. The challenges we are confronted with are outlined as: 1) how to develop a fast DSE scheme for the large-scale power systems? 2) how to better handle the nonlinearities and non-Gaussian noises of the power systems in an effective and efficient way? 3) how to develop an outlier detection algorithm for power systems which not only requires no prior knowledge of measurement outliers but also fits for online application; and 4) how to assess the estimation performance of the proposed DSE scheme?

Accordingly, the novelties of the present study are outlined in threefold: *1) a decentralized DSE scheme is proposed, which is computationally efficient and suitable for large-scale power systems; 2) a PF technique is adopted to form the core part of the decentralized DSE scheme with a view of handling nonlinearities and non-gaussian noises; 3) a novel sliding-window-based online algorithm is proposed to detect and localize the prior-knowledge-free measurement outliers; and 4) an indicator is derived to evaluate the performance of the proposed DSE algorithm.*

Notation $\|\cdot\|$ stands for the Euclidean norm of a vector. $\mathcal{N}(x|\mu,\Sigma)$ represents the Gaussian probability density function (PDF) of stochastic variable x with mean μ and covariance Σ.

2 Problem Formulation

2.1 Dynamic System Model

Consider a multi-machine power system which contains L synchronous generators (SGs). The discrete-time model of the i-th SG is given as follows [21]:

$$\delta_{i,k+1} = \delta_{i,k} + (\omega_{i,k} - \omega_s)\Delta t, \tag{1a}$$

$$\omega_{i,k+1} = \omega_{i,k} + \frac{\omega_s}{2H_i}\big[T_{mi} - P_{i,k} - D_i(\omega_{i,k} - \omega_s)\big]\Delta t, \tag{1b}$$

$$E'_{qi,k+1} = E'_{qi,k} + \frac{1}{T'_{d0,i}}\big[-E'_{qi,k} - (X_{d,i} - X'_{d,i})I_{di,k} + E_{fdi,k}\big]\Delta t, \tag{1c}$$

$$E'_{di,k+1} = E'_{di,k} + \frac{1}{T'_{q0,i}}\big[-E'_{di,k} + (X_{q,i} - X'_{q,i})I_{qi,k}\big]\Delta t \tag{1d}$$

with

$$I_{di,k} = \frac{1}{X'_{di}}(E'_{qi,k} - V_{qi,k}),\ I_{qi,k} = \frac{1}{X'_{qi}}(-E'_{di,k} + V_{di,k}),$$
$$V_{di,k} = V_{i,k}\sin(\delta_{i,k} - \theta_{i,k}),\ V_{qi,k} = V_{i,k}\cos(\delta_{i,k} - \theta_{i,k}) \tag{2}$$

where the subscripts i and k represent the SG index ($i = 1, 2, \ldots, M$) and the time instant, respectively; Δt is the discretization time step; δ and ω are, respectively, the rotor angle and speed of the SG; w_s is the nominal rotor speed; $\frac{\omega_s}{2H}$ is the inertia time instant; P is the active power injection at the terminal bus of the SG which will be given later; T_m and D are the mechanical torque input and the damping factor, respectively; E_{fd} is the field voltage; E'_d and E'_q are the dq components of the internal voltage behind a transient reactance; T'_{d0} and T'_{q0} are the dq components of the transient open-circuit time instants; X_d and X_q are the dq components of the synchronous reactance; X'_d and X'_q are the dq components of the transient synchronous reactance; I_d and I_q are the dq components of the currents; V_d and V_q are the dq components of the terminal voltage; V and θ are the terminal bus voltage magnitude and phase angle, respectively. It is worth pointing out that T_m is treated as a constant parameter in this model since the slow dynamics of the speed-governor is ignored.

In this paper, we assume that each SG is excited by the IEEE-DC1A type of automatic voltage regulator (AVR). The discrete-time model of the IEEE-DC1A AVR for the i-th SG can be written as [21]:

$$E_{fdi,k+1} = E_{fdi,k} + \frac{1}{T_{Ei}}\big[-(K_{Ei} + A_{xi}e^{B_{xi}E_{fdi,k}}) \times E_{fdi,k} + V_{Ri,k}\big]\Delta t, \tag{3a}$$

$$V_{Fi,k+1} = V_{Fi,k} + \frac{1}{T_{Fi}}(-V_{Fi,k} + \frac{K_{Fi}}{T_{Fi}}E_{fdi,k})\Delta t, \tag{3b}$$

$$V_{Ri,k+1} = V_{Ri,k} + \frac{1}{T_{Ai}}\big[-V_{Ri,k} - \frac{K_{Ai}K_{Fi}}{T_{Fi}}E_{fdi,k}$$

$$+ K_{Ai}V_{Ri,k} + K_{Ai}(V_{refi} - V_{i,k})\big]\Delta t \quad (3c)$$

where the subscripts i ($i = 1, 2, \ldots, M$) and k are the S-G index and the time instant, respectively; T_E and K_E are the exciter time instant and exciter gain, respectively; A_x and B_x represent the AVR exciter saturation constants; V_R is the scaled output of the pilot exciter; V_F is the scaled output voltage of the stabilizing transformer; T_F and K_F are, respectively, the excitation system stabilizer time instant and gain instant; K_A and T_A are AVR gain and time instant, respectively; V_{ref} and V are AVR reference voltage and terminal bus voltage magnitude, respectively.

By using the equations mentioned above, the discretized state-space model of the i-th SG can be obtained as

$$x_{i,k+1} = f_i(x_{i,k}, u_{i,k}) + w_{i,k} \quad (4)$$

where $x_{i,k} \triangleq [\delta_{i,k}\ \omega_{i,k}\ E'_{qi,k}\ E'_{di,k}\ E_{fdi,k}\ V_{Fi,k}\ V_{Ri,k}]^T \in \mathbb{R}^{n_x}$ is the state vector, $u_{i,k} \triangleq [V_{i,k}\ \theta_{i,k}]^T \in \mathbb{R}^{n_u}$ is the input vector and $f_i(\cdot)$ is determined by (1)-(3). $w_{i,k} \in \mathbb{R}^{n_x}$ is the system process noise which is allowed to be non-Gaussian in this paper.

2.2 Model Decoupling and PMU Measurement

As discussed in [23,28], there are two typical approaches to decoupling the SG model from the rest of the system model. In this paper, we regard the voltage phasors as inputs and current phasors as outputs to decouple the SG from the remaining system. Accordingly, the PMU measurement function of the i-th SG can be written as

$$f_{i,k} = f_0(w_{i,k} - w_s + 1), \quad (5a)$$
$$P_{i,k} = V_{di,k}I_{di,k} + V_{qi,k}I_{qi,k}, \quad (5b)$$
$$Q_{i,k} = -V_{di,k}I_{qi,k} + V_{qi,k}I_{di,k} \quad (5c)$$

where the subscripts i ($i = 1, 2, \ldots, M$) and k represent the SG index and the time instant, respectively; f and f_0 are the rotor frequency and the base frequency, respectively; P and Q are, respectively, the active and reactive power injections of the terminal bus. The definitions of V_d, V_q, I_d and I_q are all given in (2). Moreover, the discussion about f_k can be obtained by referring to [11].

A compact measurement model of the i-th SG can be arranged as

$$z_{i,k} = h_i(x_{i,k}, u_{i,k}) + v_{i,k} \quad (6)$$

where $z_{i,k} \triangleq [f_{i,k}\quad P_{i,k}\quad Q_{i,k}]^T \in \mathbb{R}^{n_y}$ is the measurement vector, $h_i(\cdot)$ is determined by (5), $v_{i,k} \in \mathbb{R}^{n_y}$ represents the measurement noise which is also allowed to be non-Gaussian. Throughout this paper, it is assumed that $w_{i,k}$, $v_{i,k}$ and $x_{i,0}$ are mutually independent.

2.3 Non-Gaussian Noise and Measurement Outliers

In this paper, the so-called Gaussian mixture model (GMM) is used to model the non-Gaussian distribution [1, 22], i.e.,

$$p(x) = \sum\nolimits_{i=1}^{Mc} \alpha_i \mathcal{N}_i(x|\mu_i, \Sigma_i) \quad (7)$$

where M_c is the number of Gaussian mixture components, $\mathcal{N}_i(x|\mu_i, \Sigma_i)$ is the i-th Gaussian mixture component with mean μ_i and covariance Σ_i, α_i is the weight of $\mathcal{N}_i(x|\mu_i, \Sigma_i)$ subject to $\alpha_i > 0$ and $\sum_{i=1}^{Mc} \alpha_i = 1$.

Remark 1 *As discussed in the introduction, the noises of power systems may follow non-Gaussian distributions (e.g. log-normal distribution, beta distribution and Student's t-distribution). It is shown that the GMM is a general model that can be used to represent or approximate any non-Gaussian distribution [3]. In other words, the GMM could covers various types of non-Gaussian noises, and is therefore adopted in this paper to characterize the non-Gaussian noises.*

In addition to the non-Gaussian noises, outliers constitute another source of contamination imposed on the PMU measurements. Note that outliers are not uncommon as they are likely to be generated by gross errors, cyber-attacks or large non-Gaussian noises [29]. Moreover, as compared with its centralized counterpart, the decentralized DSE are more vulnerable to outliers due to its nature of measurement redundancy, and this reinforces the importance of tackling measurement outliers.

2.4 Problem Statement

In this paper, we aim to develop a PF-based decentralized DSE algorithm for power systems that is capable of

(1) estimating the states of large-scale power systems with the aid of decentralized implementation technique;
(2) tackling nonlinearities and non-Gaussian noises of the power systems in an efficient way; and
(3) detecting and then localizing the measurement outliers in an online fashion by imbedding an improved outlier criterion into the framework of the PF.

3 Particle Filtering Method

In this section, a brief review is carried out on the PF algorithms based on the sampling importance resampling (SIR). For more details, we refer the readers to [4].

We first transform the system described by (4) and (6) into a probabilistic form as follows:

$$x_{i,k} \sim \tau_i(x_{i,k}|u_{i,k-1}, x_{i,k-1}), \quad (8)$$
$$z_{i,k} \sim \lambda_i(z_{i,k}|u_{i,k}, x_{i,k}) \quad (9)$$

where $\tau_i(\cdot)$ represents the state transition PDF and $\lambda_i(\cdot)$ is the likelihood function.

From a Bayesian point of view, the aim of the SE is to infer the posterior PDF $\pi_i(x_{i,k}|U_{i,k}, Z_{i,k})$ of the state $x_{i,k}$ with $U_{i,k} \triangleq \{u_{i,1}, u_{i,2}, \ldots, u_{i,k}\}$ and $Z_{i,k} \triangleq \{z_{i,1}, z_{i,2}, \ldots, z_{i,k}\}$.

Based on the Bayes rule, the solution to $\pi_i(x_{i,k}|U_{i,k}, Z_{i,k})$ can be obtained recursively as follows:

$$\begin{aligned}&\pi_i(x_{i,k}|U_{i,k}, Z_{i,k})\\ \triangleq&\frac{\lambda_i(z_{i,k}|u_{i,k}, x_{i,k})\pi_{i,p}(x_{i,k}|U_{i,k-1}, Z_{i,k-1})}{\rho_i(z_{i,k}|U_{i,k-1}, Z_{i,k-1})}\end{aligned} \quad (10)$$

with

$$\begin{aligned}&\pi_{i,p}(x_{i,k}|U_{i,k-1}, Z_{i,k-1})\\ \triangleq&\int \tau_i(x_{i,k}|u_{i,k-1}, x_{i,k-1})\pi_i(x_{i,k-1}|U_{i,k-1}, Z_{i,k-1})\\ &\times dx_{i,k-1},\end{aligned} \quad (11)$$

$$\begin{aligned}&\rho_i(z_{i,k}|U_{i,k-1}, Z_{i,k-1})\\ \triangleq&\int \lambda_i(z_{i,k}|u_{i,k}, x_{i,k})\pi_{i,p}(x_{i,k}|U_{i,k-1}, Z_{i,k-1})dx_{i,k}\end{aligned} \quad (12)$$

where $\pi_{i,p}(\cdot)$ and $\rho_i(\cdot)$ are, respectively, the predictive PDFs of $x_{i,k}$ and $z_{i,k}$ given $U_{i,k-1}$ and $Z_{i,k-1}$.

In practice, the recursion of the posterior PDF is only a conceptual solution from the Bayesian perspective and cannot be obtained in a closed-form. As such, in this paper, the PF approach, which can be represented by a set of random particles with associated weights, is used to approximate the posterior PDF $\pi_i(x_{i,k}|U_{i,k}, Z_{i,k})$, i.e.,

$$\pi_i(x_{i,k}|U_{i,k}, Z_{i,k}) \approx \sum\nolimits_{j=1}^{M} q_{i,k}^{(j)} \delta(x_{i,k} - x_{i,k}^{(j)}) \quad (13)$$

where M is the number of particles, $\delta(\cdot)$ is the Dirac delta function, $\{x_{i,k}^{(j)}\}_{j=1}^{M}$ is a set of particles drawn from $\pi_i(x_{i,k}|U_{i,k}, Z_{i,k})$, and $\{q_{i,k}^{(j)}\}_{j=1}^{M}$ is a set of normalized weights for the associated particles.

The steps of the SIR-based PF are outlined as follows.

1) Initialization The initial particles $\{x_{i,0}^{(j)}\}_{j=1}^{M}$ are drawn from the initial PDF $\pi_i(x_{i,0}|u_{i,0}, z_{i,0})$, and $\pi_i(x_{i,0}|u_{i,0}, z_{i,0})$ is assumed to be known previously. Moreover, the initial values of the associated weights $\{q_{i,0}^{(j)}\}_{j=1}^{M}$ are all set as $1/M$.

2) Recursion After initialization, the posterior PDF $\pi_i(x_{i,k}|U_{i,k}, Z_{i,k})$ can be estimated by propagating the particles $\{x_{i,k-1}^{(j)}\}_{j=1}^{M}$ forward in time with appropriate weights. The detailed procedures are given as follows.

2.1) One-step Prediction: In this stage, the posterior particle set $\{x_{i,k-1}^{(j)}\}_{j=1}^{M}$ at time instant $k-1$ is propagated one-step ahead to form the prior particle set $\{\bar{x}_{i,k}^{(j)}\}_{j=1}^{M}$. Specifically, the prior particle set $\{\bar{x}_{i,k}^{(j)}\}_{j=1}^{M}$ is drawn from $\tau_i(x_{i,k}|u_{i,k-1}, x_{i,k-1}^{(j)})$, i.e.,

$$\bar{x}_{i,k}^{(j)} = f_i(x_{i,k-1}^{(j)}, u_{i,k-1}) + w_{i,k-1}^{(j)}$$

where $w_{i,k-1}^{(j)}$ is a sample from the process noise.

2.2) Compute the Importance Weights: Based on the prior particle set $\{\bar{x}_{i,k}^{(j)}\}_{j=1}^{M}$, the importance weights of the SIR-based PF can be computed by resorting to the likelihood function [4, 15]. Since $z_{i,k} \in \mathbb{R}^{n_y}$, (i.e. there are n_y measurement outputs), the importance weights $\{\bar{q}_{i,k}^{(j)}\}_{j=1}^{M}$ can be rewritten as follows [8]:

$$\bar{q}_{i,k}^{(j)} = \prod\nolimits_{m=1}^{n_y} \lambda_{m,i}(z_{i,k}^{m}|u_{i,k}, \bar{x}_{i,k}^{(j)})$$

where $z_{i,k}^{m}$ is the m-th measurement output of $z_{i,k}$.

After normalization, we have

$$q_{i,k}^{(j)} = \frac{\bar{q}_{i,k}^{(j)}}{\sum_{j=1}^{M} \bar{q}_{i,k}^{(j)}}. \quad (14)$$

3) State Estimation Here, based on the prior particle set $\{\bar{x}_{i,k}^{(j)}\}_{j=1}^{M}$ and the associated weight set $\{q_{i,k}^{(j)}\}_{j=1}^{M}$, the estimate of $x_{i,k}$ can be represented as

$$\hat{x}_{i,k} = \sum\nolimits_{j=1}^{M} q_{i,k}^{(j)} \bar{x}_{i,k}^{(j)}. \quad (15)$$

4) Particles Resampling In order to avoid the particle degeneration, the SIR-based PF needs to use the resampling strategy to drop the negligible particles and duplicate the remaining particles at each iteration [4]. Specifically, in this step, a new set of particles $\{x_{i,k}^{(j)}\}_{j=1}^{M}$ is generated based on the resampling strategy where the corresponding weights are all set to be $1/M$.

4 Mechanism for Outlier Detection and Processing

As mentioned in Section 3, the implementation of the PF algorithm relies on $\tau_i(x_{i,k}|u_{i,k-1}, x_{i,k-1})$ and $\lambda_i(z_{i,k}|u_{i,k}, x_{i,k})$. Therefore, the approximation error of the posterior PDF $\pi_i(x_{i,k}|U_{i,k}, Z_{i,k})$ would be very large if the measurements are contaminated by outliers.

In this section, we aim to propose a novel online outlier detection and localization algorithm to determine whether the new arriving measurement data are contaminated by outliers. In other words, the whole measurement vector is detected first and then the specific abnormal components of the measurement vector are located and subsequently handled if the measurement vector is declared an outlier.

4.1 Outlier Detection Criterion

As studied in [17, 28], the distance criterion has been widely used in the outlier detection problems. Recently, a novel criterion, named the sequential outlier criterion (SOC), has been proposed in [27]. The SOC is achieved by calculating the expected neighbor distance and the expected neighbor direction vector through the historical data. The advantages of the SOC approach are distinct because it is suitable for online application and is also capable of dealing with data contaminated by non-Gaussian noises [27].

It should be pointed out that when it comes to the actual application scenarios, the SOC approach may face the following two foreseeable challenges: 1) the memory cost increases over time since all the historical data as well as the new arriving data have to be stored; and 2) the computation efficiency would decrease gradually with growing historical data at each iteration. In order to light the memory cost and the computation burden, in this paper, an improved sequential outlier criterion is proposed by introducing a sliding window. Moreover, an extended outlier detection algorithm based on the SOC is proposed to further detect which components of the measurement vector are outliers.

4.1.1 Outlier Detection for Whole Measurement Vector

Inspired by [27], the expected neighbor distance under the sliding window for the measurement of the i-th SG at time instant $k \geq N$ ($N \geq 0$) can be expressed as

$$\text{END\_SW}_{i,k} = \sum\nolimits_{l=k-N}^{k-2} \beta_k l d\langle z_{i,l}, z_{i,l+1}\rangle \quad (16)$$

where $\beta_k \triangleq \frac{2}{(2k-N-2)(N-1)}$, $d\langle z_{i,l}, z_{i,l+1}\rangle \triangleq \|z_{i,l+1} - z_{i,l}\|$, N is the length of the sliding window, $\beta_k l$ represents the coefficient whose value is increased when the distance is closer to the new arriving data with $\sum_{l=k-N}^{k-2} \beta_k l = 1$.

The upper bound $\text{U\_D}_{i,k}$ and the lower bound $\text{L\_D}_{i,k}$ of the expected neighbor distance under the sliding window for the measurement of the i-th SG at time instant k can be represented as

$$\begin{cases} \text{U\_D}_{i,k} = \text{END\_SW}_{i,k} + \lambda_{d,i}\sigma_{d,i,k}, \\ \text{L\_D}_{i,k} = \text{END\_SW}_{i,k} - \lambda_{d,i}\sigma_{d,i,k} \end{cases} \tag{17}$$

where $\lambda_{d,i}$ is the coefficient which determines the sensitivity of the outlier detection conditions, $\sigma_{d,i,k}$ represents the standard deviation of $d\langle z_{i,l}, z_{i,l+1}\rangle$ with $l = k-N, k-N+1, \ldots, k-2$. Finally, the new arriving measurement $z_{i,k}$ will be suspected to be an outlier if $d\langle z_{i,k-1}, z_{i,k}\rangle$ is out of the range of expected neighbor distance under the sliding window.

Remark 2 *The criterion developed in* (16) *reveals the trends of the current measuring data to some extent by resorting to the historical data contained in a sliding window whose length is N (i.e. the number of $d\langle z_{i,l}, z_{i,l+1}\rangle$ is N). Moreover, it can be found that the higher sampling rate of the sensing unit owns, the better* (16) *can reveal the trends of the current measurement. Note that it has been reported in [11, 19, 23, 29] that the PMU can better reveal the dynamic behavior of the power systems owing to its high sampling rate. As such, the criterion given in* (16) *can reveal the trends of $z_{i,k}$ (i.e. $d\langle z_{i,l}, z_{i,l+1}\rangle$ is close to $d\langle z_{i,k-1}, z_{i,k}\rangle$) due to the merits of the PMU.*

4.1.2 Outlier Localization for Specific Measurement Components

It is not difficult to find that the expected neighbor distance under the sliding window makes a "hard" decision on $z_{i,k} \in \mathbb{R}^{n_y}$ since an outlier is declared when just a few (even just one) of its components are atypical. As such, we would like to continue checking every element of $z_{i,k}$ to see if it goes out of the range of expected neighbor distance under the sliding window.

Inspired by [27], the expected neighbor direction vector under the sliding window for the measurement of the i-th SG at time instant $k \geq N$ ($N \geq 0$) can be written as

$$\begin{aligned} &\text{ENDV\_SW}_{i,k} \\ &= \begin{bmatrix} \text{ENDV\_SW}_{i,k}^1 & \text{ENDV\_SW}_{i,k}^2 & \cdots & \text{ENDV\_SW}_{i,k}^{n_y} \end{bmatrix}^T \end{aligned}$$

where

$$\text{ENDV\_SW}_{i,k}^m = \sum\nolimits_{l=k-N}^{k-2} \beta_k l \frac{(z_{i,l+1}^m - z_{i,l}^m)}{d\langle z_{i,l}, z_{i,l+1}\rangle} \tag{18}$$

with $m = 1, 2, \ldots, n_y$, N being the length of the sliding window, $\beta_k l$ is the coefficient whose value is increased when the vector is closer to the new arriving data with $\sum_{l=k-N}^{k-2} \beta_k l = 1$.

For the m-th ($m = 1, 2, \ldots, n_y$) element of $z_{i,k}$, the upper and lower bounds of $\text{ENDV\_SW}_{i,k}^m$ are defined, respectively, as

$$\begin{cases} \text{U\_V}_{i,k}^m = \text{ENDV\_SW}_{i,k}^m + \lambda_{v,i}^m \sigma_{v,i,k}^m, \\ \text{L\_V}_{i,k}^m = \text{ENDV\_SW}_{i,k}^m - \lambda_{v,i}^m \sigma_{v,i,k}^m \end{cases} \tag{19}$$

where $\lambda_{v,i}^m$ is the coefficient which determines the sensitivity of the outlier detection conditions, $\sigma_{v,i,k}^m$ represents the standard deviation of

$$\frac{z_{i,l+1}^m - z_{i,l}^m}{d\langle z_{i,l}, z_{i,l+1}\rangle}$$

with $l = k-N, k-N+1, \ldots, k-2$. Finally, the m-th element of the new arriving measurement $z_{i,k}$ will be suspected as an outlier if $(z_{i,k}^m - z_{i,k-1}^m)$ is out of the range of $\text{ENDV\_SW}_{i,k}^m$.

Remark 3 *For the outlier detection problem, some pioneering criteria have been reported in the literature, see e.g. [2, 5, 6, 16, 17, 27]. In this paper, we follow the mainstream Euclidean-distance-based criterion to develop the outlier detection and localization algorithm. Compared with the method proposed in [27], the improvements of our method lie in that: 1) the expected neighbor distance is calculated by using the historical measurement data contained in a sliding window; 2) a time-related coefficient $\beta_k l$ is utilized to assign higher weight to the distance which is closer to the new arriving data; and 3) the specific outlier-contaminated components can be localized. The merits of such improvements are outlined in threefold: 1) the memory cost and the computation burden are low since the historical measurements are contained in a sliding window with finite length; 2) the measurement outliers considered are quite general without stringent assumptions (e.g, occasionality, probability and/or intermittency); and 3) the utilization of the measuring data and the performance of the estimation can be improved since the normal components of the outlier-contaminated measurement vector are not discarded.*

Remark 4 *The upper and lower bounds given in* (17) *and* (19) *actually rely on the statistical properties of the historical measurements and the length of the sliding window. In order to enhance the flexibility of the outlier detection and localization algorithm to various measurement outliers, two coefficients (e.g. $\lambda_{d,i}$ and $\lambda_{v,i}^m$) are considered in building* (17) *and* (19). *Moreover, two aspects need to be considered in the selections of $\lambda_{d,i}$ and $\lambda_{v,i}^m$: 1) the requirements on the estimation performance in engineering practice; and 2) the resistance of the filtering algorithm to measurement outliers (since light measurement outliers may not have significant impacts on the estimation performance).*

4.2 Outlier Processing

Suppose that one or some elements of $z_{i,k}$ have been contaminated with outliers, instead of discarding the whole measurement vector straight away, we would like to make full use of the remaining normal components of $z_{i,k}$ in our proposed outlier detection and localization scheme. Moreover, the components of $z_{i,k}$, which have been declared as outliers, are replaced with the corresponding components of the previous normal measurement $z_{i,k-1}$.

In summary, the pseudocode of our proposed algorithm (against non-Gaussian noises and measurement outliers) is outlined in Algorithm 1.

5 Performance Discussion

As discussed in [30, 33], the posterior Cramér-Rao lower bound (PCRLB) developed in [24] is a commonly used criterion in evaluating the performance of the general nonlinear filter under the Bayesian framework. Note that the PCRLB is actually an offline bound whose Fisher information matrix (FIM) is obtained by taking the expectation with respect to all the system states and measurements [33]. As such, an effective yet online estimation performance indicator, namely, the conditional PCRLB developed in [30], is adopted in this paper.

Lemma 1 *[30, 33] The conditional PCRLB, which provides a lower bound on the estimation error covariance matrix, is defined by the inverse of the FIM. The FIM $J_i(x_{i,k+1}|Z_{i,k})$ can be approximated recursively via*

$$J_i(x_{i,k+1}|Z_{i,k})$$

Algorithm 1 Decentralized particle filtering algorithm against non-Gaussian noises and measurement outliers.

Initialization: Draw particles $\{x_{i,0}^{(j)}\}_{j=1}^{M}$ from the initial PDF $\pi_i(x_{i,0}|u_{i,0}, z_{i,0})$ and let the associated weights $\{q_{i,0}^{(j)}\}_{j=1}^{M}$ all equal to $1/M$. In addition, choose the length of the sliding window N and the coefficient $\lambda_{d,i}$ and $\lambda_{v,i}^{m}$ $(m = 1, 2, \ldots, n_y)$, respectively.

Recursion:

for $k = 1, 2, \ldots$ **do**
  when $k < N$, assign $N = k - 1$;
  draw prior particles $\bar{x}_{i,k}^{(j)}$ from $\tau_i(x_{i,k}|u_{i,k-1}, x_{i,k-1}^{(j)})$, $j = 1, 2, \ldots, M$;
  compute the standard deviation of $d\langle z_{i,l}, z_{i,l+1}\rangle$, $l = k-N, k-N+1, \ldots, k-2$ and obtain $\sigma_{d,i,k}$;
  compute END_SW$_{i,k}$ and its range $[\text{L\_D}_{i,k}, \text{U\_D}_{i,k}]$ according to (16) and (17), respectively;
  compute $d\langle z_{i,k}, z_{i,k-1}\rangle$;
  if $d\langle z_{i,k}, z_{i,k-1}\rangle \notin [\text{L\_D}_{i,k}, \text{U\_D}_{i,k}]$ **then**
    $z_{i,k}$ is an outlier;
    for $m = 1$ to n_y **do**
      compute the standard deviation of $(z_{i,l+1}^{m} - z_{i,l}^{m})/d\langle z_{i,l}, z_{i,l+1}\rangle$, $l = k-N, k-N+1, \ldots, k-2$ and obtain $\sigma_{v,i,k}^{m}$;
      compute ENDV_SW$_{i,k}^{m}$ and its range $[\text{L\_V}_{i,k}^{m}, \text{U\_V}_{i,k}^{m}]$ based on (18) and (19);
      compute $(z_{i,k}^{m} - z_{i,k-1}^{m})$;
      if $(z_{i,k}^{m} - z_{i,k-1}^{m}) \notin [\text{L\_V}_{i,k}^{m}, \text{U\_V}_{i,k}^{m}]$ **then**
        the m-th element of $z_{i,k}$ (i.e. $z_{i,k}^{m}$) is an outlier;
        replace $z_{i,k}^{m}$ with the previous normal measurement $z_{i,k-1}^{m}$;
      else
        $z_{i,k}^{m} = z_{i,k}^{m}$;
      end if
    end for
    compute the normalized importance weights $\{q_{i,k}^{(j)}\}_{j=1}^{M}$ according to (14);
    compute the estimate $\hat{x}_{i,k}$ by using (15);
    resample to obtain the new particle set $\{x_{i,k}^{(j)}\}_{j=1}^{M}$.
  else
    compute the normalized importance weights $\{q_{i,k}^{(j)}\}_{j=1}^{M}$ according to (14);
    compute the estimate $\hat{x}_{i,k}$ by using (15)
    resample to obtain the new particle set $\{x_{i,k}^{(j)}\}_{j=1}^{M}$.
  end if
end for

$$\approx D_{i,k}^{22} - D_{i,k}^{21}\big(D_{i,k}^{11} + J_i\big(x_{i,k}|Z_{i,k-1}\big)\big)^{-1} D_{i,k}^{12} \qquad (20)$$

where

$$D_{i,k}^{11} \approx \frac{1}{M}\sum\nolimits_{j=1}^{M} g_{i,1}(x_{i,k}^{(j)}, x_{i,k+1}^{(j)}),$$

$$D_{i,k}^{12} \approx \frac{1}{M}\sum\nolimits_{j=1}^{M} g_{i,2}(x_{i,k}^{(j)}, x_{i,k+1}^{(j)}),$$

$$D_{i,k}^{22} \approx \frac{1}{M}\sum\nolimits_{j=1}^{M} g_{i,3}(x_{i,k}^{(j)}, x_{i,k+1}^{(j)}) + \frac{1}{M}\sum\nolimits_{j=1}^{M} g_{i,4}(x_{i,k+1}^{(j)})$$

and

$$g_{i,1}(x_{i,k}, x_{i,k+1})$$

$$= \frac{\nabla_{x_{i,k}}\tau_i(x_{i,k+1}|u_{i,k}, x_{i,k})\nabla_{x_{i,k}}^{T}\tau_i(x_{i,k+1}|u_{i,k}, x_{i,k})}{\tau_i^2(x_{i,k+1}|u_{i,k}, x_{i,k})},$$

$$g_{i,2}(x_{i,k}, x_{i,k+1})$$

$$= \frac{\nabla_{x_{i,k}}\tau_i(x_{i,k+1}|u_{i,k}, x_{i,k})\nabla_{x_{i,k+1}}^{T}\tau_i(x_{i,k+1}|u_{i,k}, x_{i,k})}{\tau_i^2(x_{i,k+1}|u_{i,k}, x_{i,k})},$$

$$g_{i,3}(x_{i,k}, x_{i,k+1})$$

$$= \frac{\nabla_{x_{i,k+1}}\tau_i(x_{i,k+1}|u_{i,k}, x_{i,k})\nabla_{x_{i,k+1}}^{T}\tau_i(x_{i,k+1}|u_{i,k}, x_{i,k})}{\tau_i^2(x_{i,k+1}|u_{i,k}, x_{i,k})},$$

$$g_{i,4}(x_{i,k}, x_{i,k+1})$$

$$= \int \frac{\nabla_{x_{i,k+1}}\lambda_i(z_{i,k+1}|u_{i,k}, x_{i,k})\nabla_{x_{i,k+1}}^{T}\lambda_i(z_{i,k+1}|u_{i,k}, x_{i,k})}{\lambda_i(z_{i,k+1}|u_{i,k}, x_{i,k})} \times dz_{i,k+1}$$

with $x_{i,k}^{(j)}$ $(j = 1, \ldots, M)$ *representing the particles and* $\nabla_{x_{i,k+1}}$ *denoting the operator of the first order partial derivative given by* $\nabla_{x_{i,k+1}} = \left[\frac{\partial}{\partial x_{i,k+1}^{1}}, \cdots, \frac{\partial}{\partial x_{i,k+1}^{n_x}}\right]^{T}$. *Note that the close-form solution to* $g_{i,4}(x_{i,k}, x_{i,k+1})$ *is hard to be obtained and one can resort to some alternative approaches to approximate such a solution. Moreover, the initial value of the conditional PCRLB is set as* $J_i(x_{i,0}|z_{i,-1}) = J_i(x_{i,0})$.

Proof: The proof of Lemma 1 is readily accessible from [30, 33], and is thus omitted here. □

Remark 5 *Until now, an efficient decentralized DSE scheme has been developed for power systems against non-Gaussian noises and measurement outliers. As compared to the existing algorithms in the literature for similar purposes, the main results established in this paper stand out for the following reasons: 1) a fast DSE scheme for the large-scale power systems is proposed, which can be implemented at each SG by using the local PMU measurements; 2) the core element of the decentralized DSE scheme is the particle filtering technique, which is particularly effective in handling nonlinearities as well as non-Gaussian noises; 3) a novel online sliding-window-based detection and localization algorithm, which is embedded into the decentralized DSE algorithm, is proposed to tackle the measurement outliers; and 4) the conditional PCRLB for the proposed DSE algorithm is derived.*

6 Simulation Experiments

In this section, the simulation studies are conducted on the IEEE 39-bus system to verify the performance of the proposed algorithm. The detailed parameters of the IEEE 39-bus system are taken from [13], and all simulations continue for 25s. The collections of frequency, active power injection and reactive power injection at each generator's terminal bus are treated as PMU measurements. The sampling rate of the PMU is assumed to be 100 samples/s. Due to the limitation of the space, only the states of SG 3 are taken for illustration purposes. The initial estimate of SG 3 is set as $\hat{x}_{3,0} = [0.9\ 0.5\ 0.1\ 0.45\ 1\ 0\ 1]^{T}$. For the selections of other simulation parameters, we follow the common used trial-and-error method by fully considering the number of particles, length of the sliding window and the accuracy of the outlier detection and localization. The root mean square error (RMSE), defined by $\text{RMSE} = \sqrt{\frac{1}{n_x}\sum_{i=1}^{n_x}\left(x_{i,k} - \hat{x}_{i,k}\right)^2}$ with n_x representing

the number of state variables, is chosen as overall estimation performance index.

6.1 Scenario 1: Gaussian and Non-Gaussian Noises

In this scenario, two cases are considered as follows.

Case 1 : A zero-mean Gaussian white sequence with covariance matrix $10^{-6}I$ is used to characterize the process and measurement noises.

Case 2 : The GMM-based non-Gaussian sequences are used to simulate the process and measurement noises, i.e. $w_{3,k} \sim 0.9\mathcal{N}_1(0, 10^{-6}I) + 0.1\mathcal{N}_2(0, 10^{-4}I)$ and $v_{3,k} \sim 0.9\mathcal{N}_1(0, 10^{-6}I) + 0.1\mathcal{N}_2(0, 10^{-4}I)$.

For the purpose of testifying our proposed scheme, comparisons between the generalized maximum-likelihood-type (GM) based UKF proposed in [9, 28] (labeled as R-UKF) and the SIR-based particle filter (labeled as SIR-PF) with different number of particles are carried out. Moreover, the corresponding conditional PCRLB for the SIR-PF is also calculated. The simulation results are shown in Figs. 1-2.

From Figs. 1 and 2, we can find that: 1) for the SIR-PF, the estimation accuracy is increased with the growing number of particles; 2) for the Gaussian noises, the estimates provided by the R-UKF are more accurate than that of the SIR-PF; 3) for the non-Gaussian noises, the RMSEs of the R-UKF and the SIR-PF are almost the same; and 4) the RMSE of the SIR-PF is close to the CPCRLB.

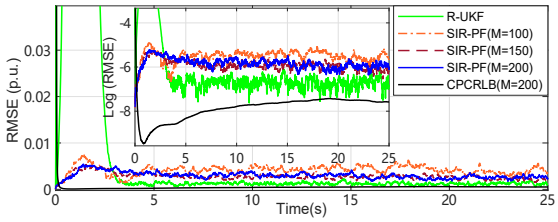

Fig. 1. Scenario 1: RMSE of Generator 3 under Case 1.

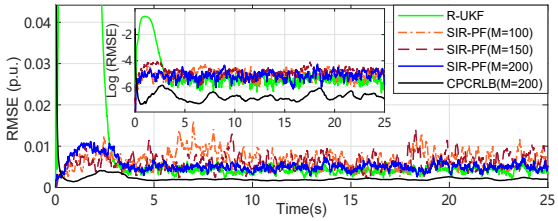

Fig. 2. Scenario 1: RMSE of Generator 3 under Case 2.

6.2 Scenario 2: Outliers Caused by Gross Errors

In this scenario, a zero-mean Gaussian white sequence with covariance matrix $10^{-6}I$ is used to characterize the process and measurement noises. In order to evaluate the performance of our proposed outlier detection particle filter (labeled as OD-PF), the following two cases are considered:

Case 1 : The terminal measurements of Generator 3 are contaminated with instantaneous gross errors. Specifically, 1) when $t = 8$s, f_3 is contaminated with 0.4% error; 2) when $t = 12$s, P_3 and Q_3 are corrupted with 5% errors; and 3) when $t = 16$s, f_3, P_3 and Q_3 are corrupted with 1%, 2% and 3% errors, respectively.

Case 2 : The terminal measurements of Generator 3 are contaminated with consecutive gross errors. Specifically, 1) from $t = 8$s to $t = 8.1$s, f_3 and P_3 are corrupted with 0.4% and 50% errors, respectively; and 2) from $t = 12$s to $t = 13$s, f_3, P_3 and Q_3 are contaminated with 4%, 20% and 30% errors, respectively.

The simulation results under case 1 are shown in Figs. 3 and 4, respectively. Specifically, Fig. 3 shows the RMSEs of the R-UKF, the OD-PF (with different M and N) and the SIR-PF as well as the CPCRLB for the OD-PF, respectively. The outlier detection and localization results as well as the estimation results are plotted in Fig. 4(a) and 4(b), respectively. Similarly, the results under case 2 are shown in Figs. 5 and 6, respectively.

From Figs. 3-6, we can conclude that: 1) for the OD-PF, the estimation accuracy is improved with the growing number of particles and the increasing length of the sliding-window; 2) the RMSEs of the R-UKF and the OD-PF are almost the same in the presence of instantaneous gross error; 3) when the consecutive gross error occurs, the OD-PF performs much better than the R-UKF and the SIR-PF; 4) the measurement outlier caused by the instantaneous or consecutive gross error can be detected and localized accurately with the proposed algorithm; and 5) the RMSE of the OD-PF is close to the CPCRLB.

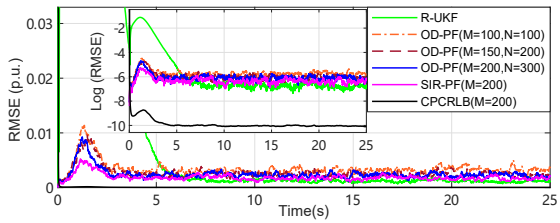

Fig. 3. Scenario 2: RMSE of Generator 3 under Case 1.

6.3 Scenario 3: Outliers Caused by Non-Gaussian Noises

In order to test the performance of the proposed OD-PF to the measurement outliers caused by the non-Gaussian noises, in this scenario, a zero-mean Gaussian white sequence with covariance matrix $10^{-6}I$ is still used to characterize the process and measurement noises and: 1) from $t = 8$s to $t = 8.1$s, f_3 is corrupted by a GMM-based non-Gaussian sequence with distribution $0.3\mathcal{N}_1(1, 10^{-1}I) + 0.7\mathcal{N}_2(0, 10^{-6}I)$; and 2) from $t = 12$s to $t = 13$s, f_3, P_3 and Q_3 are contaminated by a GMM-based non-Gaussian sequence with distribution $0.8\mathcal{N}_1(0.5, 10^{-4}I) + 0.2\mathcal{N}_2(0.2, 10^{-3}I)$.

The simulation results are plotted in Figs. 7 and 8. Specifically, the RMSEs of the R-UKF, the OD-PF and the SIR-PF as well as the CPCRLB for the OD-PF are given in Fig. 7, respectively. Fig. 8(a) and 8(b) show the outlier detection and localization results as well as the estimation results, respectively.

It can be confirmed from Figs. 7 and 8 that: 1) the estimation accuracy of the OD-PF is improved with the growing number of particles and the increasing length of the sliding-window; 2) when the non-Gaussian-based outlier occurs, the OD-PF performs much better than the R-UKF and the SIR-PF; 3) when the process and measurement noises are Gaussian, the measurement outlier caused by the non-Gaussian noise can be precisely

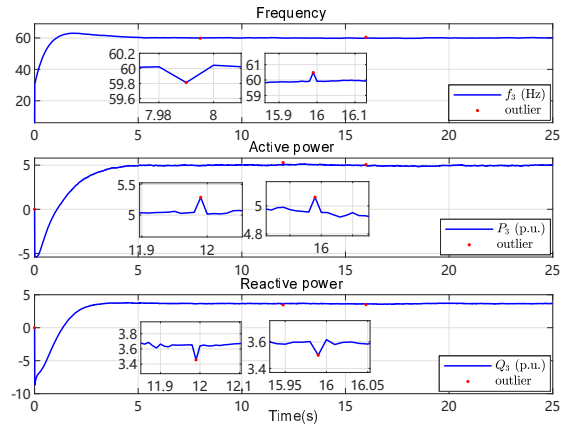

(a)

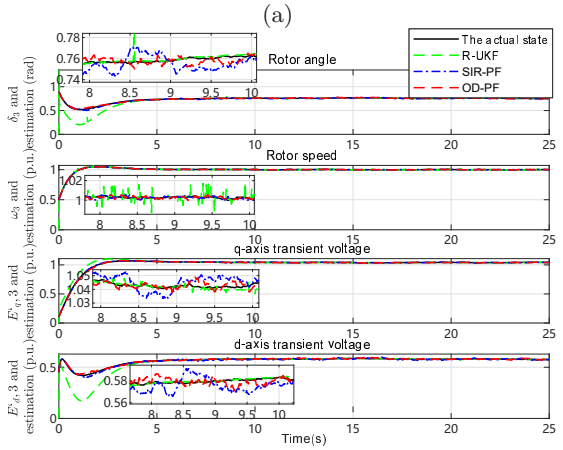

(b)

Fig. 4. Scenario 2: Estimation results of Generator 3 under Case 1 ($M = 200, N = 300$): (a) Outlier detection and localization. (b) Estimated states.

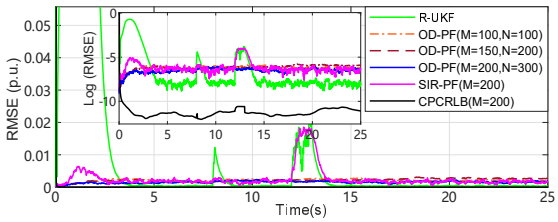

Fig. 5. Scenario 2: RMSE of Generator 3 under Case 2.

detected and localized by using our proposed OD-PF algorithm; and 4) the RMSE of the OD-PF is close to the CPCRLB.

6.4 Scenario 4: Computational Efficiency

Table 1
Average Computing Time Under Three Scenarios At Each PMU Scan

Scenario	1		2		3
Item	Case 1	Case 2	Case 1	Case 2	outliers caused by non-Gaussian noise
ACTs	3.10 ms	3.50 ms	5.08 ms	4.82 ms	4.87 ms

In this scenario, the computational efficiencies of the former scenarios are discussed. All the test cases are implemented on a PC with Intel Core CPU i7-7700HQ, 2.80GHz and 16 GB RAM. The average computing times

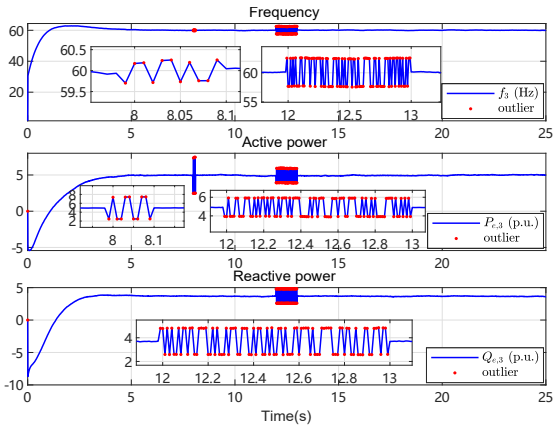

(a)

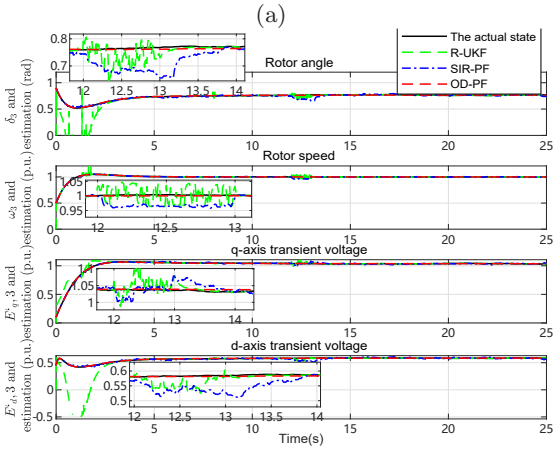

(b)

Fig. 6. Scenario 2: Estimation results of Generator 3 under Case 2 ($M = 200, N = 300$): (a) Outlier detection and localization. (b) Estimated states.

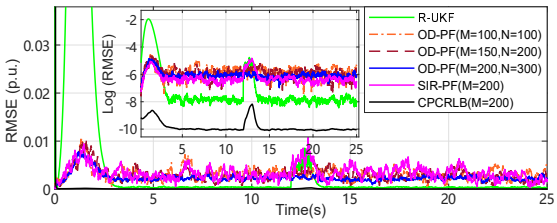

Fig. 7. Scenario 3: RMSE of Generator 3.

(ACTs) of the above three scenarios are presented in Table 1. From Table 1, we can conclude that: 1) the proposed decentralized DSE algorithm has high computational efficiency since the average computing times of each iteration are much lower than the PMU scan rate (10 ms/sample); and 2) the proposed DSE scheme is able to track the dynamic systems of the power systems in real-time.

7 Conclusion

In this paper, we have investigated the decentralized DSE problem for large-scale power systems with non-Gaussian noises and measurement outliers. A model decoupling approach has been adopted to enable the DSE in a decentralized manner for the purpose of lighting the computation burden and increasing the algorithm execution efficiency. In order to better tackle the nonlineari-

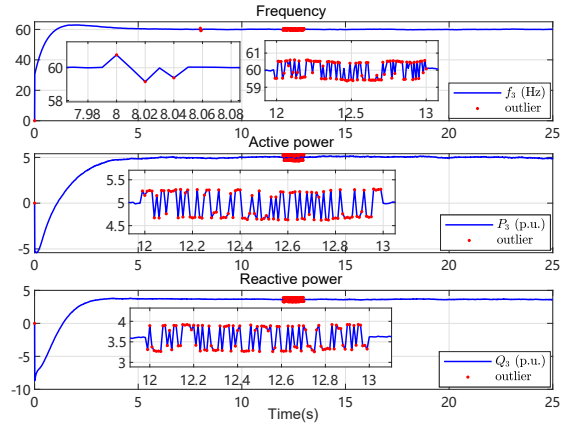

(a)

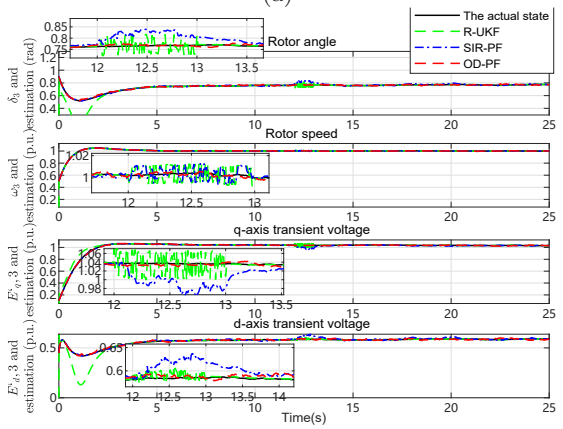

(b)

Fig. 8. Scenario 3: Estimation results of Generator 3 ($M = 200, N = 300$): (a) Outlier detection and localization. (b) Estimated states.

ties as well as the non-Gaussian noises, the PF technique has been applied to achieve the decentralized DSE. To achieve the detection and localization of the measurement outliers, an online sliding window-based algorithm is incorporated into the particle filter. The performance of the proposed DSE algorithm is assessed by using the conditional PCRLB. Finally, based on the IEEE 39-bus test system, four test scenarios have been given to show the effectiveness of the proposed algorithm. An interesting yet challenging topic for future research would be to develop rigorous theoretical analysis framework for assessing the particle filtering algorithm under non-Gaussian noises and measurement outliers.

References

[1] Ahmad, T., & Senroy, N. (2020). Statistical characterization of PMU error for WAMS based analytics, *IEEE Transactions on Power Systems*, 35(2), 920–928.

[2] Alessandri, A., & Awawdeh, M. (2016). Moving-horizon estimation with guaranteed robustness for discrete-time linear systems and measurements subject to outliers, *Automatica*, 67, 85–93.

[3] Arasaratnam, I., Haykin, S., & Elliott, R. J. (2007). Discrete-time nonlinear filtering algorithms using Gauss-Hermite quadrature, in *Proceedings of The IEEE*, 95(5), 953–977.

[4] Arulampalam, M., Maskell, S., Gordon, N., & Clapp, T. (2002). A tutorial on particle filters for online nonlinear/non-Gaussian Bayesian tracking, *IEEE Transactions on Signal Processing*, 50(2), 174–188.

[5] Belsley, D. A., Kuh, E., & Welsch, R. E. (1980). Regression diagnostics: Identifying influential data and sources of collinearity. New York, NY, USA: Wiley.

[6] Cook, R. D. (2000). Detection of influential observation in linear regression, *Technometrics*, 42(1), 65–68.

[7] Debs, A. S., & Larson, R. E. (1970). A dynamic estimator for tracking the state of a power system, *IEEE Transactions on Power Apparatus and Systems*, 89(7), 1670–1678.

[8] Emami, K., Fernando, T., Iu, H. H.-C., Trinh, H., & Wong, K. P. (2015). Particle filter approach to dynamic state estimation of generators in power systems, *IEEE Transactions on Power Systems*, 30(5), 2665–2675.

[9] Gandhi, M., & Mili, L. (2010). Robust Kalman filter based on a generalized maximum-likelihood-type estimator, *IEEE Transactions on Signal Processing*, 58(5), 2509–2520.

[10] Geng, H., Liu, H., Ma, L., & Yi, X. (2021). Multi-sensor filtering fusion meets censored measurements under a constrained network environment: advances, challenges and prospects, *International Journal of Systems Science*, 52(16), 3410–3436.

[11] Ghahremani, E., & Kamwa, I. (2016). Local and wide-area PMU-based decentralized dynamic state estimation in multi-machine power systems, *IEEE Transactions on Power Systems*, 31(1), 547–562.

[12] Hu, J., Zhang, H., Liu, H., & Yu, X. (2021), A survey on sliding mode control for networked control systems, *International Journal of Systems Science*, 52(6), 1129–1147.

[13] IEEE PES TF on Benchmark System for Stability Controls,(2015). Benchmark systems for small-signal stability analysis and control, IEEE Power Energy Society, Piscataway, New Jersey, USA, Technical Report, PES-TR18.

[14] Liu, Q., Wang, Z., He, X., and Zhou, D. H. (2018). On Kalman-consensus filtering with random link failures over sensor networks, *IEEE Transactions on Automatic Control*, 63(8), 2701–2708.

[15] Li, W., Wang, Z., Yuan, Y., & Guo, L. (2020). Two-stage particle filtering for non-Gaussian state estimation with fading measurements, *Automatica*, 115, art. no. 108882.

[16] Maronna, R. A., Martin, R. D., & Yohai, V. J. (2006). Statistics: Theory and Methods, Wiley Series in Probability and Statistics. Chichester, UK: Wiley.

[17] Maíz, C. S., Molanes-López, E. M., Míguez, J., & Djurić, P. M. (2012). A particle filtering scheme for processing time series corrupted by outliers, *IEEE Transactions on Signal Processing*, 60(9), 4611–4627.

[18] Mao, J., Sun, Y., Yi, X., Liu, H., & Ding, D. (2021). Recursive filtering of networked nonlinear systems: A survey, *International Journal of Systems Science*, 52(6), 1110–1128.

[19] Qu, B., Wang, Z., & Shen, B. (2021). Fusion estimation for a class of multi-rate power systems with randomly occurring SCADA measurement delays, *Automatica*, vol 125, art. no. 109408.

[20] Sagan, A., Liu, Y., & Bernstein, A. (2021). Decentralized low-rank state estimation for power distribution systems, *IEEE Transactions on Smart Grid*, 12(4), 3097–3106.

[21] Sauer, P. W., & Pai, M. (1997). Power System Dynamics and Stability, Englewood Cliffs, NJ, USA: Prentice-Hall

[22] Song, W., Wang, Z., Wang, J., Alsaadi, F. E., & Shan, J. (2021). Secure particle filtering for cyber-physical systems with binary sensors under multiple attacks, *IEEE System Journal*, 16(1), 603–613.

[23] Singh, A. K., & Pal, B. C. (2018). Decentralized dynamic state estimation in power systems using instrument transformers, *IEEE Transactions on Signal Processing*, 66(6), 1541–1550.

[24] Tichavský, P., Muravchik, C. H., & Nehorai, A. (1998). Posterior Cramér-Rao bounds for discrete-time nonlinear filtering, *IEEE Transactions on Signal Processing*, 46(5), 1386–1396

[25] Valverde, G., Saric, A. T., & Terzija, V. (2013). Stochastic monitoring of distribution networks including correlated input variables, *IEEE Transactions on Power Systems*, 28(1), 246–255.

[26] Wang, S., Zhao, J., Huang, Z., & Diao, R. (2018). Assessing Gaussian assumption of PMU measurement error using field data, *IEEE Transactions on Power Delivery*, 33(6), 3233–3236.

[27] Zhang, S., Cao, H., Yang, S., Zhang, Y., & Hei, X. (2018). Sequential outlier criterion for sparsification of online adaptive filtering, *IEEE Transactions on Neural Networks and Learning Systems*, 29(11), 5277–5291.

[28] Zhao, J., & Mili, L. (2018). Power system decentralized dynamic state estimation based on multiple hypothesis testing, *IEEE Transactions on Power Systems*, 33(4), 4553–4562.

[29] Zhao, J., Gomez-Exposito, A., Netto, M., Mili, L., Abur, A., Terzija, V., Kamwa, I., Pal, B. C., Singh, A. K., Qi, J., Huang, Z., & Meliopoulos, A. P. S. (2019). Power system dynamic state estimation: Motivations, definitions, methodologies, and future work, *IEEE Transactions on Power Systems*, 34(4), 3188–3198.

[30] Zheng, Y., Ozdemir, O., Niu, R., & Varshney, P. K. (2012), New conditional posterior Cramér-Rao low bounds for nonlinear sequential Bayesian estimation, *IEEE Transactions on Signal Processing*, 60(10), 5549–5556.

[31] Zhou, N., Meng, D., Huang, Z., & Welch, G. (2015), Dynamic state estimation of a synchronous machine using PMU data: A comparative study, *IEEE Transactions on Smart Grid*, 6(1), 450–460.

[32] Zou, L., Wang, Z., Hu, J., & Dong, H. (2022). Ultimately bounded filtering subject to impulsive measurement outliers, *IEEE Transactions on Automatic Control*, 67(1), 304–319.

[33] Zuo, L., Niu, R., & Varshney, P. K. (2011). Conditional posterior Cramér-Rao lower bounds for nonlinear sequential Bayesian estimation, *IEEE Transactions on Signal Processing*, 59(1), 1–14.